



# RAINFALL ENERGY CHARACTERIZATION IN CUYAGUATEJE BASIN EROSION

## Caracterización energética de las precipitaciones en la erosión de la cuenca del Cuyaguaje

**Yeleine Almoza Hernández<sup>1</sup>✉, Wim M. Cornelis<sup>2</sup>, Hanoi Medina González<sup>1</sup>,  
Maria E. Ruiz Pérez<sup>1</sup>, Gustavo Alonso Brito<sup>1</sup>, Jorge Díaz Suarez<sup>1</sup>  
and Donald Gabriels<sup>2</sup>**

**ABSTRACT.** In Cuba, one of the prioritized regions in terms of water erosion is “Cuyaguaje” river basin, where more than 85 % of its soil shows a high erosion risk subjected to intensive farming practices. High pluviometric values registered together with the non-uniform topography necessitate spatially characterised rain erosivity in this area, as it constitutes an essential factor of soil erosion. The objectives of this paper were: (a) to compare expressions that predict kinetic energy from rainfall intensity in our basin of interest, (b) to develop and validate the relationship between cumulative rainfall and R factor from RUSLE (Revised Universal Soil Loss Equation) ( $EI_{30}$ ), (c) to compare results and trends between R and the Modified Fournier Index MFI, as well as with Lal’s index  $AI_m$  ( $EI_{7.5}$ ), (d) to present rainfall erosivity maps, according to each index calculated. Data from two pluviographic stations were used to calculate R (by Brown and Foster’s also Kinnell’s kinetic energy equations) and  $AI_m$ , besides data from 26 pluviometric stations located along the basin of interest. Thus, R values ranged between 8284 and 22044 MJ mm ha<sup>-1</sup> h<sup>-1</sup>yr<sup>-1</sup> through both kinetic energy equations, with the highest erosivity values at the top or mountainous part and the lowest values at the basin bottom. Around 96 % of the basin area is affected by rainfall with high erosive potential. Correlations between R factor from RUSLE and the other indexes calculated (MFI and  $AI_m$ ) were higher than 0,9.

**RESUMEN.** En Cuba, una de las regiones priorizadas en términos de erosión hídrica es la cuenca del río Cuyaguaje, donde más del 85 % de su suelo presenta alto riesgo de erosión por estar bajo intensas prácticas de laboreo. Los altos acumulados de precipitaciones registrados junto a la no uniformidad de la topografía hacen necesaria una caracterización espacial de la erosividad de las lluvias en el área, ya que constituye un factor fundamental de la erosión. Los objetivos de este trabajo fueron: (a) comparar expresiones que estiman la energía cinética, desde la intensidad de las precipitaciones en la cuenca bajo estudio; (b) desarrollar y validar la relación entre los acumulados de precipitación y el factor R del Modelo RUSLE (Ecuación de Perdidas de Suelo Universal Revisada) ( $EI_{30}$ ); (c) comparar resultados y tendencias entre R y el Índice Modificado de Fournier MFI así como con el Índice de Lal,  $AI_m$  ( $EI_{7.5}$ ); (d) presentar los mapas de erosividad de las precipitaciones, según cada índice calculado. Fueron utilizados datos de dos estaciones pluviográficas de la cuenca para calcular R (usando las ecuaciones de energía cinética de Brown y Foster y la de Kinnell) y  $AI_m$  y datos de 26 estaciones pluviométricas a lo largo de toda la cuenca. Como resultado se obtuvo valores de R entre 8284 y 22044 MJ mm ha<sup>-1</sup> h<sup>-1</sup>yr<sup>-1</sup> mediante las dos ecuaciones de energía cinética, con los valores más elevados de erosividad en la parte alta o montañosa y los valores más bajos en la parte baja de la cuenca. Alrededor del 96 % del área de la cuenca está afectada por las precipitaciones con alto potencial erosivo. Las correlaciones entre el factor R de RUSLE y el resto de los índices calculados (MFI y  $AI_m$ ) fueron altas, más de 0,9.

**Key words:** kinetic energy, intensity, rainfall, soil erosion

**Palabras clave:** energía cinética, intensidad, precipitaciones, erosión del suelo

## INTRODUCTION

Since the 1980’s, many scientific works related with soil erosion have been developed, especially with rainfall influence on this process. So far, some

<sup>1</sup> Universidad Agraria de la Habana, Grupo de Investigaciones Agrofísicas, Autopista Nacional km 23 y 1/2, San José de las Lajas, Mayabeque, Cuba.

<sup>2</sup> Ghent University, Department of Soil Management, Coupure links 653, Ghent, Belgium.

✉ madehp@infomed.sld.cu

authors (1, 2) like those from India (3) have developed new RS-GIS based on simple methods for estimating bank erosion. This method does not need intense field investigation and can provide erosion vulnerability zonation near to rivers.

The most serious environmental problem in Cuba is soil degradation, which is to a great extent due to the high erosivity of rainfall events<sup>A</sup>. CITMA reported that about 70 % of the arable area suffers from soil degradation, and approximately 43 % of this area is subjected from medium to strong water erosion.

A program directed to promote sustainable management of hydrographic watersheds, particularly those of major social, economic and environmental importance, was established more than a decade ago. One of the prioritized regions is "Cuyaguaje" basin, which belongs to the eight most important basins of the country and is located in the western part of Cuba (West of Havana). A considerable area of "Cuyaguaje" basin has been strongly eroded according to the Sciences Academy of Cuba<sup>B</sup>. Recently, rough estimates indicated that 22 % of the total basin area or 86 % of the arable land showed a very high erosion risk under the current land use practices (4).

Some widely adopted tools in establishing erosion control plans are erosion models, which enable to indicate actual and potential erosion problem areas, and estimate the effect of control measures through scenario analysis (5, 6). There is a variety of erosion models since USLE (7) RUSLE (5) and others more complex like WAST (8). These models have been mainly developed based on statistical methods or from empirical observations.

Empirical models have generally a simpler structure, require less input parameters and often show more similar performance in terms of prediction accuracy than deterministic models, when considering yearly averages, and show a low degree of error propagation according to other works carried out (9). RUSLE (Revised Universal Soil Loss Equation) empirical model estimates soil loss by taking into account factors like topography, soil erodibility, vegetation, soil management and rainfall erosivity ( $R$  factor). Because of its wide use and simplicity, this model has been chosen for erosion risk assessment in "Cuyaguaje" basin (4).

Erosion risk assessment depends, however, to a great extent on the proper spatial and temporal characterization of rainfall erosivity. Various studies suggest the relationship between rainfall and the response in terms of erosion is determined not only by the cumulative rainfall but also by some measurements of raindrop fall velocity.

Combining the latter with drop diameter, provided by drop-size distribution measurements, kinetic energy or time has been proposed as indicators for rainfall erosivity. Some authors proposed to multiply kinetic energy  $E$  with a measure of maximum rainfall intensity (5), the maximum being 30-minute rainfall intensity  $I_{30}$ , which is known as  $EI_{30}$ . This parameter corresponds to  $R$  factor erosivity in (R) USLE. Intensity values can be derived from pluviographic data.

Determining rainfall kinetic energy from the size and fall velocity of each raindrop comprising the event is impractical; therefore, parameterizations have been developed to deduce it empirically from intensity data. Examples of such relationships applicable for various regions are given (10–12).

The rain kinetic energy (KE). In reviewing studies from 19 locations worldwide (12) found that  $E-I$  relationship established (1) based on data from Miami FL, USA (which is supposed to have a similar climate as in our study area, western Cuba) was substantially different (10 %) from the relationships presented by others (9), based on data from Washington DC, USA and used in USLE (2) based on data from Holly Springs MS, USA and used in RUSLE (5) when compared with storm energy data (24 storms) collected in Gunnedah, Southeast Australia (13). In the same study (1, 12)  $E-I$  relationship differed with almost 15 % from a generalized equation they derived after re-examining those different datasets from around the world.

The higher  $E$  estimates derived for subtropical humid Florida were primarily associated with the high kinetic energy content predicted at low rainfall intensities (12). The same authors further argued that exponential  $E-I$  relationships, like others (1, 2) are better suited than power or logarithmic relations. It should be noted that  $E$  relationships represents the amount of kinetic energy expended per unit of rain volume (1, 2).

<sup>A</sup>Alonso, G. *Magisterial Conference of the President of Cuban Agency of Environment*. (entr. Almoza H. Y.), [Personal Communication], 2011, VII Congress of Cuban Soil Science, La Habana, Cuba.

<sup>B</sup>Cuban Academic of Science. *Hydraulic of Cuyaguaje Watershed*. La Habana, Cuba, 2010, pp. 12-20.

However, the researcher argued (11) that it is statistically more appropriate to express  $E$  in terms of kinetic energy expended per unit area and per unit time for fitting with  $I$ . They also demonstrated that when considering existing drop-size distribution models, it is most suitable to link the time-specific  $E$  and  $I$  with a power law. Such power law expression was used (14) to estimate time-specific  $E$  for Florida, USA.

Apart from spatial differences following geographic location and rain type (11), temporal differences in storm erosivity are common. For example, in “Dos Quebradas” basin region, in the central coffee growing region of Colombia,  $EI_{30}$  was calculated with an annual precipitation of 2,600–3,200 mm. With this research work, it was found that individual storms represented as much as 25 % of the annual  $EI_{30}$  (10,409–15,975 MJ mm ha<sup>-1</sup> h<sup>-1</sup> yr<sup>-1</sup>) and observed marked differences between wet and dry season erosivity models.

To circumvent the necessity of kinetic energy for computing erosivity, Lal index,  $AI_m$  (15), derived from Nigerian data can be used. It is the product of rainfall amount per storm with maximum 7,5-minute intensity.

However, intensity data needed to derive  $R$  and  $AI_m$  are not often available on a high resolution scale. Therefore, other erosivity indices have been introduced. A popular index is the Modified Fournier Index (16), MFI, originally developed for Morocco. MFI is the sum of the monthly precipitation squared over annual precipitation; however, many authors concluded that, MFI, represents a poor erosivity index. Alternatively, models have been developed that predict  $R$  from rainfall amount, for instance in Mediterranean area (17–19), in Nigeria (15, 20), Iran (21, 22), Kenya (23, 24) and Spain (15). Differences in model parameters suggest, however, that these relationships are sites or specific regions (15).

The overall objective of this study was to assess spatial and temporal erosivity in “Cuyaguaje” river basin in the western part of Cuba. As in most regions around the world, pluviographic data in quiet long time series and sufficiently high special resolution are rare to allow spatial interpolation. The specific objectives of this work were: (a) to compare expressions that predict kinetic energy from rainfall intensity relevant for our basin of interest, (b) to develop and validate a region-specific relation between RUSLE  $R$  and rainfall amount available from pluviometric stations, (c) to compare trends in  $R$  with MFI and  $AI_m$  and (d) to present erosivity maps based on the above indicators.

## MATERIAL AND METHODS

### STUDIED AREA

“Cuyaguaje” river basin has an area of 723 km<sup>2</sup> with a total river length of 112.4 km from its origin at “Cabras hill” down to its mouth at the Caribbean Sea<sup>c</sup>. The basin is located in Pinar del Río province in western Cuba (Figure 1).

The watershed is, as the rest of Cuba, subjected to a subtropical climate. A well-defined dry season lasts from November to April, with a mean annual rainfall of 1766 mm; a mean annual temperature of 25,1 °C varying from 22,0 °C in January to 27,7 °C in July and August; its relative humidity is around 77 % in the dry season and around 82 % during the rest of the year (rainy season).

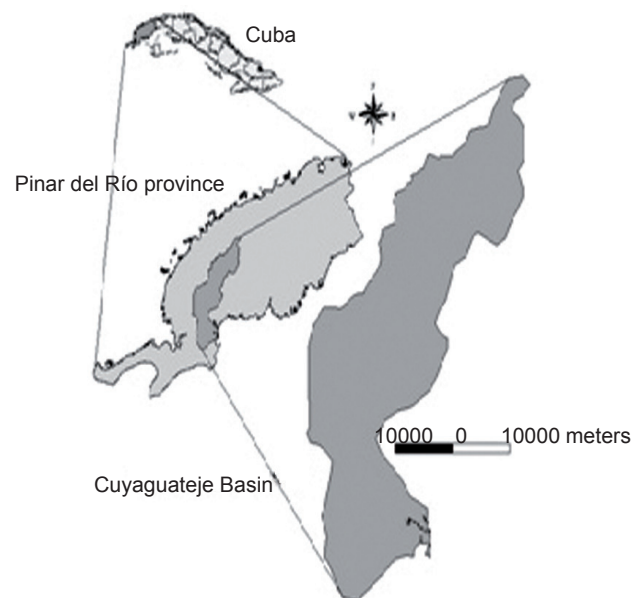


**Figure 1. Location of Cuyaguaje river basin at the west part of Cuba**

“Cuyaguaje” river watershed is characterized by an anticline chain of mountains named “Cordillera de Guaniguanico”. In its northern part, the mountain range “Sierra de los Órganos” is characterized by steep sided limestone hills and numerous cultivated valleys. This karstic region has undergone very intensive geological erosion and has an extensive subterranean drainage system. At both sides of this range, “Alturas de Pizarras” forms a hill landscape that is also severely eroded and its poorly developed soils are composed of slate, schist and sandstone. The southern part of the watershed is characterized by a sandy lowland plain called “Llanura costera sur”. The elevation varies from 0 to 589 m at sea level, with an average elevation of 124 m<sup>c</sup>.

<sup>c</sup> INRH. *Catálogo de Cuencas Hidrográficas Río Cuyaguaje*. Inst. National Institute of Hydraulic Resources, Cuba, 2014, p. 6.

According to soil map (scale 1:25000) from Cuban Soil Institute, the main soil types in the region are Ferralsols and Leptosols<sup>c</sup>. The land is mainly cultivated with tobacco, beans, maize, fallow and pine forests (*Pinus caribea* L. and *Pinus tropicalis* (4).

### RAINFALL RECORDS

Daily rainfall data of 20 six pluviometric stations were available, but only three of them provided pluviographic data as well. All pluviometric and pluviographic data were recorded by the National Institute of Water Resources (INRH). Data series length, location, altitude, position and mean annual rainfall are shown in Table I. The spatial distribution over the watershed is shown in Figure 2. Only the years with complete rainfall records were retained, which resulted in lengths per station varying between 1965 and 1992. The stations with pluviographic data used were "V Aniversario" (station 122; 1964-1992) and Portales II (station 334; 1964-1992). It is also important to remark that after 1990's economic crisis in Cuba, it was stopped to gradually measure those rainfall records in the experimental stations. Up-to-date registrations do not exist. At present, INRH is working on it.

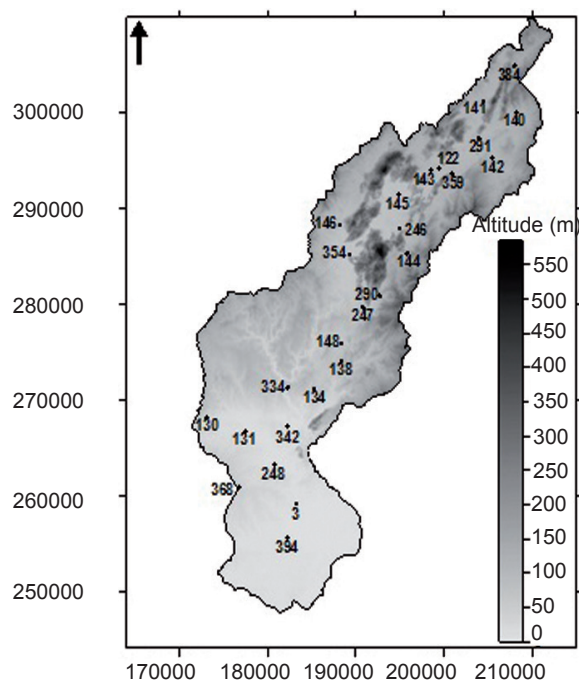


Figure 2. Distribution of pluviometric station along Cuyaguajeje river basin

Table I. Location, station number, record length, Cuba plane coordinates system of the pluviometric stations at Cuyaguajeje watershed

Location	Station No.	Record length (years)	Altitude (m)	X Cuba north coordinates, East (m)	Y Cuba north coordinates, North (m)
La Catalina	3	22	10	183591	259224
V Aniversario	122	29	90	199402	294227
La Deseada	130	30	40	173106	268122
Asiento Viejo	131	28	15	177498	266733
Las Cañas	134	29	70	185208	271128
Cayo Borrego	138	29	105	188302	274019
Isabel Maria	140	29	110	208206	300119
Quemado de Pineda	141	29	120	204397	301237
Finca El Mulo	142	29	102	205398	295219
Pica Pica	143	22	90	198542	293941
José Marti	144	29	200	195796	285314
San Laureano	145	29	85	194802	291517
Santiago Puente	146	29	100	188188	288326
Santa Lutgarda	148	29	80	188395	275832
Correo San Carlos	246	27	80	194989	287914
Correo Punta de la Sierra	247	28	60	190792	279722
Isabel Rubio	248	28	10	180807	263219
La Majagua	290	28	105	192790	280912
Los Aguados	291	21	105	203894	297340
E.A. Portales II	334	27	90	182290	271310
Guane	342	55	20	182293	267219
E.A. La Guira	354	24	70	189299	285227
Sumidero	359	17	110	200906	293613
Puesto de Mando D.A.P	368	21	50	176803	260841
Granja Moncada	384	18	200	208011	304922
Cuyaguajeje E.C.	394	16	40	182197	255530



**KINETIC ENERGY-RAINFALL INTENSITY RELATIONSHIPS**

In RUSLE manual (6) the exponential equation is suggested (2) to calculate the kinetic energy  $e_k$  per pluvio-phase  $k$  ( $\text{MJ ha}^{-1} \text{mm}^{-1}$ ), from the rain intensity  $i_k$  in the pluvio-phase  $k$  ( $\text{mm h}^{-1}$ ):

$$e_k = 0,29 [1 - 0,72 \exp(-0,05i_k)] \quad (\text{Equation 1})$$

As it is said, this equation was established using data from Mississippi, USA, which suggests for Florida, USA (1) an equation with similar shape but different in its parameters:

$$e_k = 0,2931 [1 - 0,281 \exp(-0,018i_k)] \quad (\text{Equation 2})$$

Smith and De Veaux (14) suggest for Florida, USA:

$$e_k = 0,11 i_k^{0,14} \quad (\text{Equation 3})$$

Other authors (12) presented a general equation after re-examining datasets from 19 locations all over the world taken from literature. Those data well represented a variety of climates and geographic regions, and resulted in:

$$e_k = 0,28 [1 - 0,52 \exp(-0,042i_k)] \quad (\text{Equation 4})$$

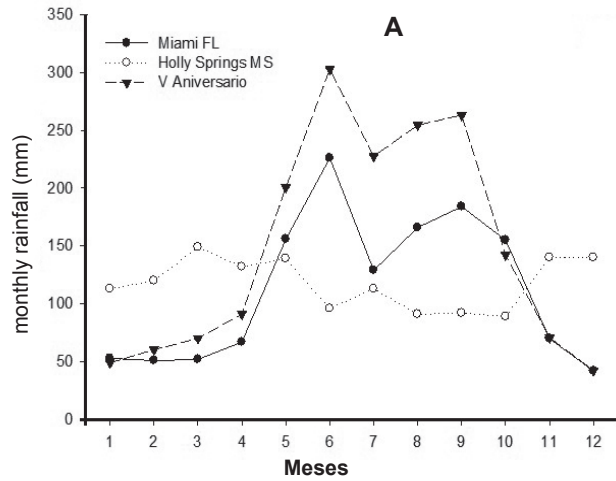
Also others (11) presented a universal equation, with model parameters depending upon rain type by considering the existing drop-size distribution models from literature. For convective storm, which are typically occurring in Cuba (25), they suggested:

$$e_k = 0,1351 i_k^{0,1608} \quad (\text{Equation 5})$$

The reason for selecting two equations for Florida, USA is that it exhibits a climate rather similar to the one in the studied area. Figure 3a shows monthly rainfall distribution at “V Aniversario” station for 1964-1992 (data from INRH, Cuba), as well as at Holly Springs MS, USA and Miami FL, USA for 1961-1991 (data from FAOclim version 2,02; 26). “V Aniversario” (90 m altitude) and Miami FL (4 m altitude) show very similar rainfall patterns, but the former showed higher rainfall amounts. Figure 3b shows monthly temperature at the same locations, with temperatures for “V Aniversario” taken from FAOclim version 2.02 as well (nearby “Minas Matahambre” station, 13 years). Also, a high resemblance between Miami FL and “V Aniversario” can be observed.

Based on the above rainfall and temperature data, both the climate at “V Aniversario” and Miami FL can be classified as Aw (tropical savanna). Although medium drop size and hence kinetic energy have been related to temperature, its effect may also reflect differences in storm type (12).

**Monthly rainfall distribution at the V Aniversario station and others places**



**Monthly mean temperature**

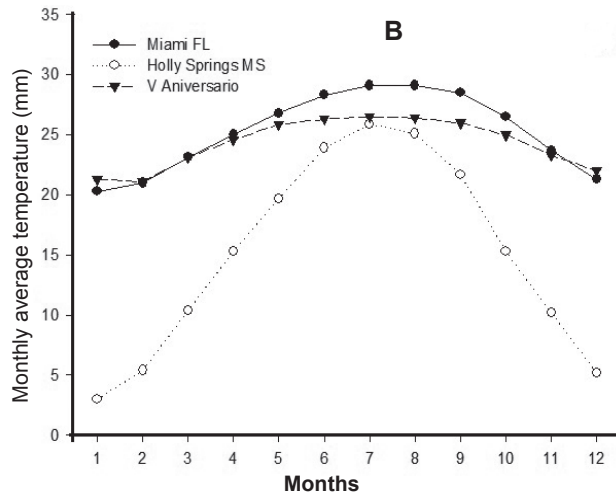


**Figure 3. Comparative diagram of some climate characteristics**

Furthermore, wind speed and altitude affect kinetic energy of rain storms. Wind shear not only changes drop-size distribution of a storm (16) it also affects the impact energy of drops at the surface causing detachment

It can finally be noted here that Equation (5) was developed using drop-size data (27) obtained with a drop-camera technique for five rain types (air mass, pre-cold front, warm front, easterly wave and trough aloft), which are also typically occurring in the studied area<sup>C</sup>. Intuitively, we could therefore assume that the equation 2 is the best option to predict kinetic energy in western Cuba.

Before deducing RUSLE-R for the three pluviographic stations (see section 2.4),  $e_k$  was first computed with Equations 1-5 for the 11550 pluvio-phases, corresponding with storms observed

at "V Aniversario" (station 122) within 1964-1992. The obtained  $e_k$  values were then used to estimate individual storm  $EI_{30}$  values (using Equation 7, section 2.4), which were finally employed for comparing  $E-I$  models and selecting the most appropriate one for western Cuba.

### RUSLE-R EROSION FACTOR FOR THE PLUVIOGRAPHIC STATIONS

RUSLE  $R$  erosion factor was calculated for the pluviographic stations as equation 6.

$$R = \frac{1}{n} \sum_{i=1}^n \left( \sum_{j=1}^m (EI_{30})_j \right)_i \quad (\text{Equation 6})$$

where:

$R$ : the averaged erosivity in  $n$  years expressed in  $\text{MJ mm ha}^{-1} \text{h}^{-1}$

$m$ : the number of rain events each year

$i$ : the year

$j$ : is a rain event

$EI_{30}$  is the erosivity of a rain event expressed in  $\text{MJ mm ha}^{-1} \text{h}^{-1}$  individual storm  $EI_{30}$  values were calculated from (5).

$$EI_{30} = \left( \sum_{k=1}^q e_k \Delta V_k \right) I_{30} \quad (\text{Equation 7})$$

where:

$E$ : the total kinetic energy of a rain event expressed in  $\text{MJ ha}^{-1}$

$I_{30}$ : the maximum intensity of a rainfall during 30 minutes in  $\text{mm}$

$q$ : the number of pluvio-phases of the rain event

$e_k$ : is the kinetic energy by unit of rain amount and surface in pluvio-phase  $k$  in  $\text{MJ ha}^{-1} \text{mm}^{-1}$

$\Delta V_k$ : is the amount of rain in the pluvio-phase  $k$  in  $\text{mm}$

As it is suggested (7) rain events of less than 12,7 mm were omitted in calculating annual  $R$  factor, unless at least 6,35 mm of rain fell in 15 minutes.

RUSLE  $R$  values by event ( $EI_{30}$ ) were computed using software programmed in C language that produces a file with: 1) event number, 2) event beginning, 3) event end, 4) rainfall by event, 5) maximum intensity of a rainfall during 30 minutes by event, 6) maximum intensity of a rainfall for seven minutes, 7) kinetic energy by event and finally, 8) RUSLE  $R$  factor by event.

### RUSLE-R EROSION FACTOR FOR ALL STATIONS

Daily  $R$  erosion factors  $R_d$  were obtained by adding  $EI_{30}$  values corresponding to all the events on a daily basis. At the same time, rainfall corresponding to

each event was summarized to daily totals  $P_d$ .  $R_d$  and  $P_d$  were grouped by months to evaluate the temporal effect of erosivity within the year.

Rather than pooling all data from the three pluviographic stations to regress daily  $R$  against daily  $P$ , data were only considered for "V Aniversario". This station was selected as it comprised the longest time series (29 years). The relationships developed for "V Aniversario" was then validated for the two other pluviographic stations, one of which was located within the same sub-watershed. Since the three pluviographic stations had incomplete intensity records, but complete daily rainfall data, these expressions were then used not only to compute daily erosivity values  $R_d$  of the remaining 23 pluviometric stations, but also to recalculate daily erosivity values for the three pluviographic stations (using pluviometric data available at those stations). A similar procedure was followed to obtain monthly  $R_m$  and annual  $R$  values for each of the stations.

### MODIFIED FOURNIER INDEX (MFI)

The Modified Fournier index  $MFI$  is defined as (15):

$$MFI = \frac{\sum_{i=1}^{12} P_i^2}{P} \quad (\text{Equation 8})$$

where:

$P_i$ : is the mean rainfall in  $\text{mm}$  of month  $i$

$P$ : is the mean annual rainfall ( $\text{mm}$ ). It was calculated for every station ( $n=26$ ) and compared with annual  $R$ .

### LAL EROSION INDEX

Some authors (16) introduced an index that can be written as:

$$AI_m = 100 \sum_{i=1}^{12} \left( \sum_{j=1}^n (P_d I_{\max} \tau)_j \right)_i \quad (\text{Equation 9})$$

where:

$AI_m$  is rain erosivity, expressed in  $\text{cm}^2 \text{h}^{-1}$

$I_{\max 7}$  is the maximum rainfall intensity of seven minutes in  $\text{mm h}^{-1}$

$n$  is the number of rain events in the month.

The same methodology used for determining monthly  $R$  values was applied, but considering rainfall maximum intensity at seven minutes, rather than at 30 minutes.

## MAPPING EROSIVITY

Interpolation is a method or mathematical function that estimates the values at locations where no measured values are available. Interpolation can be as simple as a number line; however, most geographic information science research involves spatial data. Spatial interpolation assumes the attribute data are continuous over space. Maps for each of the indexes were made using an Inverse Distance to the Square interpolation method with Surfer 7.0. Inverse Distance Weighting (IDW) is based on the assumption that the nearby values contribute more to the interpolated values than distant observations. In other words, for this method the influence of a known data point is inversely related to the distance from the unknown location that is being estimated. The advantage of IDW is that it is intuitive and efficient. This interpolation works best with evenly distributed points. Similar to the SPLINE functions, IDW is sensitive to outliers.

## RESULTS AND DISCUSSION

### KINETIC ENERGY-RAINFALL INTENSITY RELATIONSHIPS IN “V ANIVERSARIO” STATION

Pluviographic data recorded at “V Aniversario” station for 1964-1992 period yielded 2668 storms. Plotting the amount of kinetic energy expended per unit volume of rain, denoted by  $e_{kmm}$ , as a function of rainfall intensity shows large differences between  $E-I$  models (Figure 4a,b) for the intensities in the basin under study.

Exponential models all tapered off at a maximum value at intensities around  $70 \text{ mm h}^{-1}$ . Some authors (12) said there is a substantial evidence that a ‘maximum’ medium drop size is reached at intensities above  $70\text{-}100 \text{ mm h}^{-1}$ . For lower intensities than  $30 \text{ mm h}^{-1}$ , differences between those models were very substantial. However, although 92 % of our pluvio-phases had  $I \leq 30 \text{ mm h}^{-1}$ , the choice of  $E-I$  model will have a minor impact as these lower intensities are generally associated with low rainfall depths (18).

Figure 5 shows that  $EI_{30}$  values, as obtained from Miami models (Equations 2-3), are plotted against those values obtained from the reference ‘RUSLE’  $EI_{30}$  and ‘general’ equations (Equations 1 and 4-5, respectively). Over our complete dataset,  $EI_{30}$  values estimated with equation for Miami FL (2) appear to be higher than those calculated from ‘RUSLE’ equation (1).

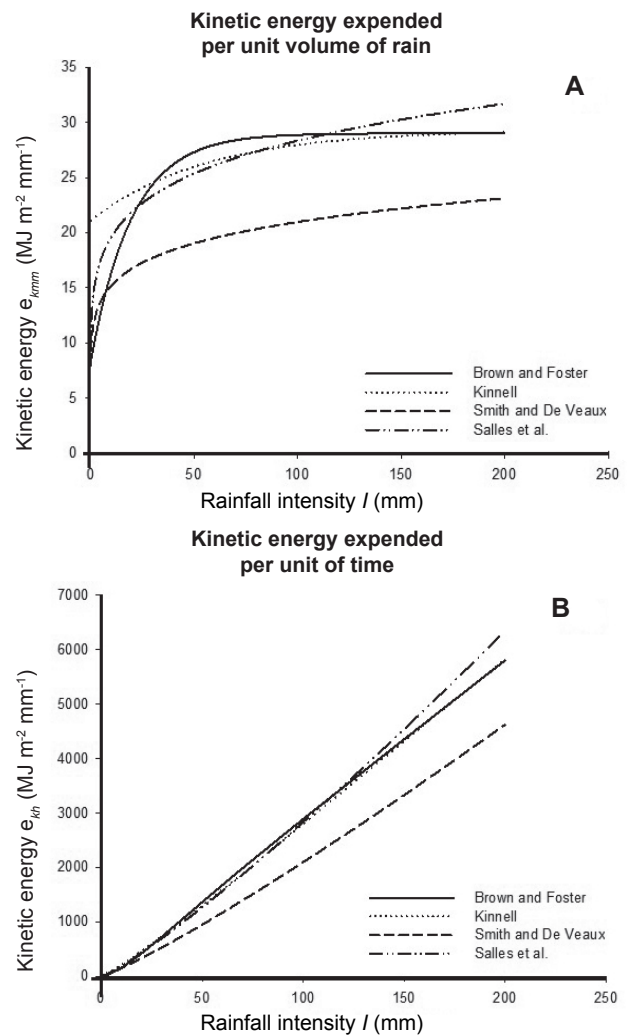


Figure 4. Kinetic energy

The largest deviations are observed for the highest  $EI_{30}$  values. They are associated with extreme duration storms ( $>22$  hours, 1,2 % of storms) and thus extreme rainfall depth ( $>200 \text{ mm}$ , 0,2 %), but somewhat less extreme  $I_{30}$  values ( $>40 \text{ mm h}^{-1}$ , 7,5 %).  $EI_{30}$  values obtained for Miami FL (14) are surprisingly much lower than those computed (2). This could have been expected from Figure 4. However, the reason for this discrepancy is not clear. Maybe a typing error of the intercept in Equation (3) could explain this large difference. Both ‘general’ equations suggested (11, 12) respectively have an intermediate position between (1) and (2) models.

When expressing kinetic energy per unit area and per unit time,  $e_{kh}$ , with the latter being equal to  $e_{kmm} i_k$ , and plotting it against rainfall intensity, differences between the models appear to be smaller (Figure 4a,b), which made (11) to conclude that  $e_{kh}$  is more appropriate to be linked to  $i_k$  than  $e_{kmm}$ .

However, *in se*, differences between both ways of expressing kinetic energy remain the same, but in the case of  $e_{k,h}$ , such differences seem to be masked by low intensities that go along with large deviations in kinetic energy that appear to exist between models at lower intensities than  $30 \text{ mm h}^{-1}$ .

The relative difference in annual  $R$  between (1) model, on one hand, and (2, 11, 12, 14) models, on the other hand, were respectively 4,4 %, 28,0 %, 4,6 % and 4,7 %. The small differences between (1) model and (2) may be surprising. According to the authors (13), using data from Southeast Australia, found a difference of 23 % between both.

A possible explanation for these small differences might be that for some very extreme storms, data might be missing in our study. During “Alberto” storm in 1982, the technician responsible for “V Aniversario” station had to escape from there, because water was rising so high as “Cuyaguaje” river was bursting its banks. Just before he left he made a last rainfall recording of 620 mm.

Although differences in annual  $R$  between (1) model and (2) were relatively small (smaller than expected), we decided to continue with another model performed (1), which was developed using data from Miami FL; as it was demonstrated earlier in this paper, it represents rainfall conditions relatively well in our studied area.

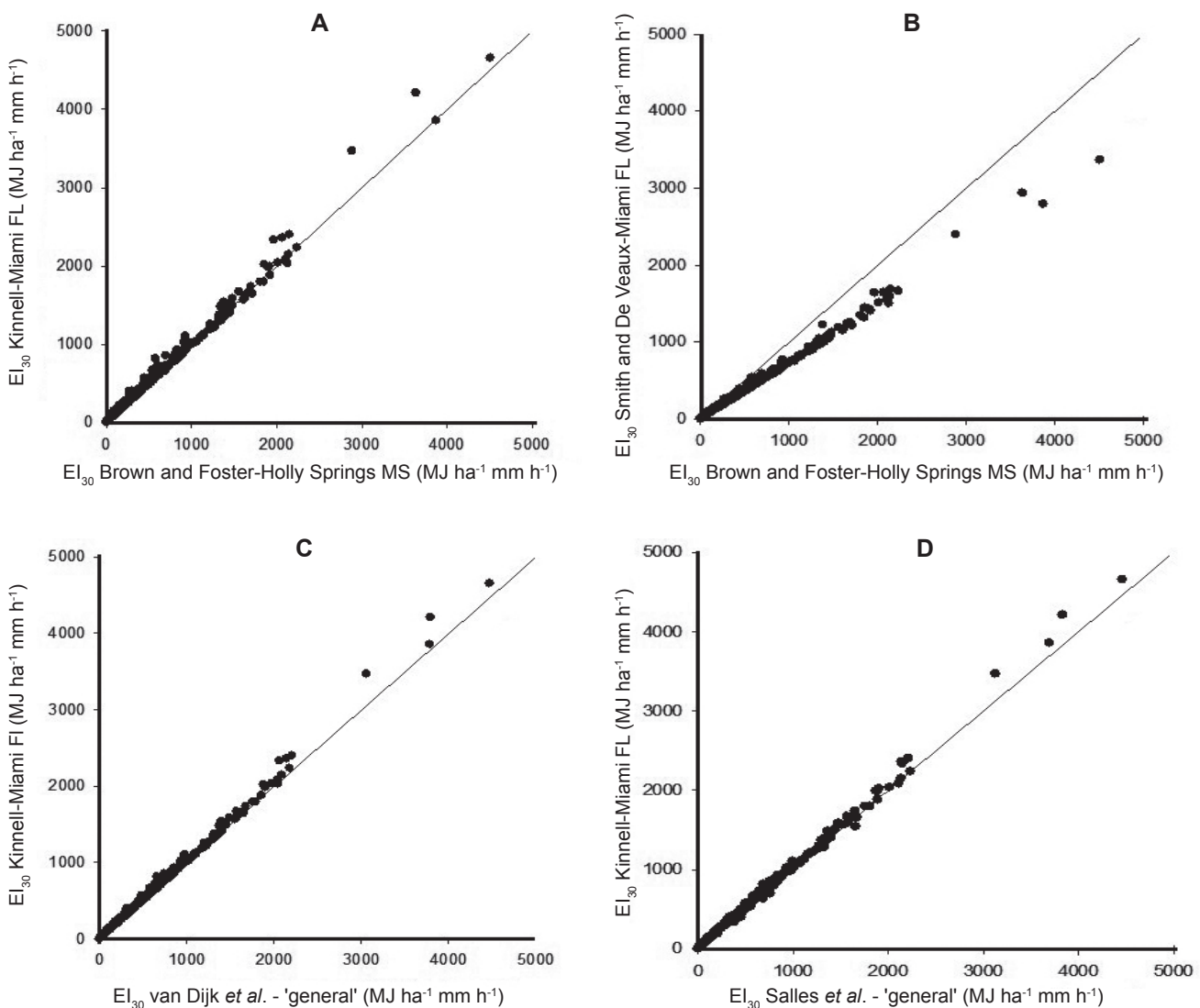


**Figure 5.** EI30 values obtained from different models of kinetic energy. a) and b)with Brown and Foster, c) and d) with general models



**EROSIVITY—RAINFALL AMOUNT RELATIONSHIPS**

The variation observed in daily erosivity was to a great extent explained by daily rainfall depth. We found that a power law well described the relation between daily  $R$  and daily  $P$  for each month. However, this equation was shown to overestimate  $R_d$  for days with  $P_d$  exceeding 70 mm (extreme events). For such days, a linear equation exhibited the best fits. Thus, it was found:

$$R_d = \alpha P_d^b \text{ for } P_d \leq 70 \text{ mm} \quad (\text{Equation 10})$$

$$R_d = c P_d + d \text{ for } P_d > 70 \text{ mm} \quad (\text{Equation 11})$$

Because of the high variation in monthly rainfall (Figure 3a), Equation (10) was fitted for each month. This yielded, according to an ANOVA test, better results than when pooling data into a wet and dry season, or over a complete year. In contrast to this, solving Equation (11) over a yearly dataset did not yield worse results than when splitting dataset into seasons or months. The same type of regression equations was obtained between daily Lal erosivity index  $AI_{md}$  and  $P_d$ :

$$AI_{md} = \alpha P_d^\beta \text{ for } P_d \leq 70 \text{ mm} \quad (\text{Equation 12})$$

$$AI_{md} = \chi P_d + \delta \text{ for } P_d > 70 \text{ mm} \quad (\text{Equation 13})$$

In  $R_d$  and  $P_d$  relationship, firstly calculating  $R_d$  by using pattern of kinetic energy (2) and later with pattern (1), all of this to be able to obtain two erosivity values for the whole basin, to compare them and finally mapping it.

Table II shows  $a$ ,  $b$ ,  $\alpha$  and  $\beta$  values obtained for each month (Equations 10 and 12), ‘annual’  $c$ ,  $d$ ,  $\chi$  and  $\delta$  values (Equations 11 and 13) and their standard errors, as well as the regression determination coefficients.

**Table II. Parameters  $a$ ,  $b$ ,  $\alpha$  and  $\beta$  obtained for each month and appearing in the potential equation between  $R_d$  and  $P_d$  and  $AI_{md}$  and  $P_d$  respectively**

Months	$R_d$ (2)			$AI_{md}$ (16)			$R_d$ (1)		
	$R_d = \alpha P_d^b$			$AI_{md} = \alpha P_d^\beta$			$R_d = \alpha P_d^b$		
	$a$	$b$	$r^2$	$\alpha$	$\beta$	$r^2$	$a$	$b$	$r^2$
January	0,136	1,986	0,9528	0,031	1,764	0,9251	0,1807	2,0891	0,9408
February	0,182	1,942	0,9515	0,034	1,696	0,9176	0,2583	1,8800	0,9027
March	0,188	2,040	0,9557	0,034	1,735	0,9477	0,2633	2,3445	0,9217
April	0,189	2,079	0,9714	0,034	1,774	0,9423	0,2613	2,0321	0,9481
May	0,188	2,040	0,9557	0,034	1,724	0,9412	0,344	1,9339	0,8733
June	0,184	2,094	0,9630	0,033	1,794	0,9462	0,2948	2,0047	0,9013
July	0,201	2,119	0,9713	0,036	1,816	0,9472	0,5743	1,8369	0,9360
August	0,212	2,084	0,9655	0,039	1,752	0,9433	0,4253	1,982	0,9409
September	0,202	2,084	0,9659	0,943	1,778	0,9433	0,8928	1,6756	0,8935
October	0,187	2,046	0,9626	0,036	1,747	0,9401	0,7375	1,7363	0,9149
November	0,159	2,001	0,9474	0,029	1,719	0,909	0,1834	1,4949	0,9279
December	0,170	1,968	0,9518	0,032	1,701	0,9242	0,1916	1,5423	0,8847

It can be noted that  $b$  and  $\beta$  values of Equations (10 and 12) for all patterns were between 2 and 1,70 for all months. The  $a$  and  $\alpha$  coefficients showed a non-stationary pattern with the lowest values from November to January (Table II).

The highest values were found from July to September for all patterns, although these months have lower precipitation than June. The latter month showed similar  $a$  and  $\alpha$  values than February, March, April, May and October, although these months exhibit rather different rainfall patterns. This means that *per mm of rain*, the three summer months show a substantially higher erosivity than the rest of the months. The lowest erosivity per mm of rain occurs from November till January. We did not capture the temporal pattern of  $a$  and  $\alpha$  in a mathematical expression. Similar conclusions could be drawn when considering Lal’s  $AI_m$  index.

In humid Nigeria, an  $a$  value of 0.27 and a  $b$  value of 1,94 were calculated with  $R$  computed from RUSLE approach as well (5) resulting in a similar erosive power per mm of rain as in our studied area (20).

The regression equations obtained above for “V Aniversario” station were validated for “Portales II” station (334) localized at 182290 Coordinate East and 271310 Coordinate North (south basin part).

“Portales II” is the station with pluviographic data located to the south. Just only four stations exist with pluviographic data inside the watershed. The validation was carried out under R pattern (2). Figure 6 shows a good agreement between  $R_m$  calculated values and those predicted with Equations 10 and 12, with  $R^2= 0,66$ , although it is not very high, but it responds satisfactorily to the estimate. In fact, it evidently proved those rainfall amounts can be or not influenced by altitude (meter), but it is not a decisive factor in the behaviour of the same one.

In Figure 7 a), the behaviour of these two variables is observed and the slight tendency to increase from north to south the rainfall means. In axis "x", the north coordinates of the 26 stations were represented whereas in axes "y" the precipitations and heights corresponding to each station. However, in Figure 7 b), a low lineal relationship is evident with  $R^2=0.41$  among height and annual rainfall amount.

**TEMPORAL AND SPATIAL BEHAVIOR OF  $R$  IN "CUYAGUATEJE" WATERSHED**

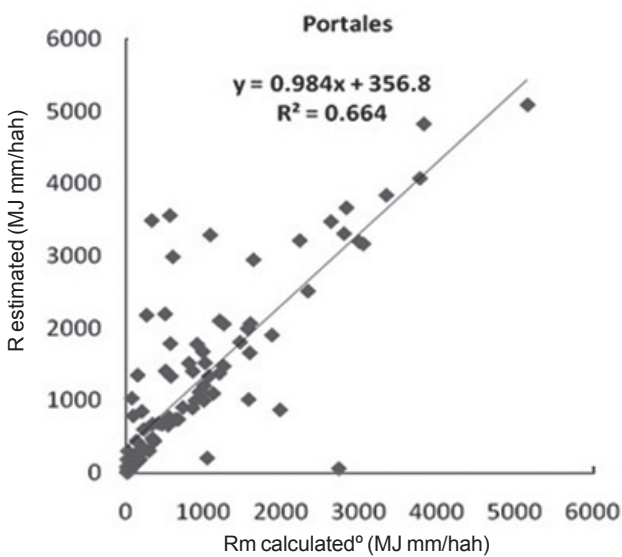
Unlike erosivity per mm of rain (that is, coefficient  $a$  in Equation 10), monthly erosivity  $R_m$  followed monthly rainfall distribution very well, with a correlation

coefficient of 0.98 between both. June is the most erosive month with a mean  $R_m$  value of 2,423  $MJ\cdot mm\cdot ha^{-1}\cdot h^{-1}$  (2) and 2,748  $MJ\cdot mm\cdot ha^{-1}\cdot h^{-1}$  (1), while December is the least erosive (mean  $R_m=171,1$  and 279,9  $MJ\cdot mm\cdot ha^{-1}\cdot h^{-1}$  respectively) (Figure 8). The high erosivity of June rainfall is not due to a higher erosivity per mm of rain, as mentioned above, but to higher amounts of rainfall, thereby higher monthly kinetic energy. Such results are important in planning agricultural and irrigation activities for minimizing soil erosion. Also, monthly  $Al_m$  followed a similar pattern and was well correlated to  $P_m$  ( $r=0,90$ ) and to  $R_m$  (1) ( $r=0,97$ ) and  $R_m$  (2) (0,96).

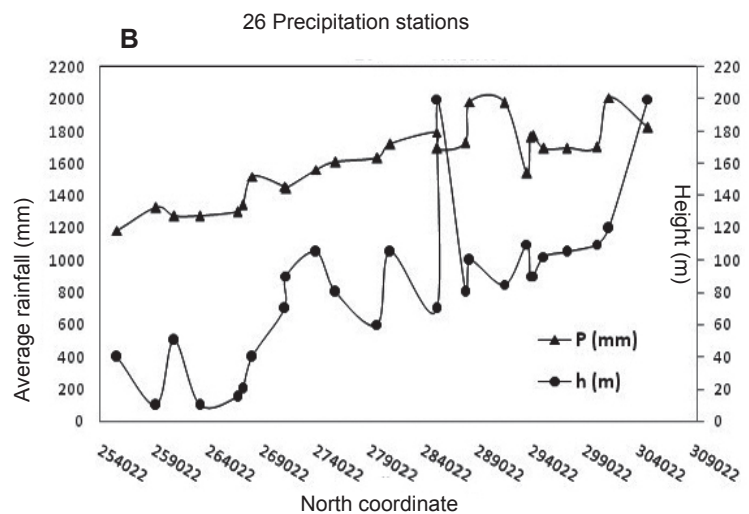
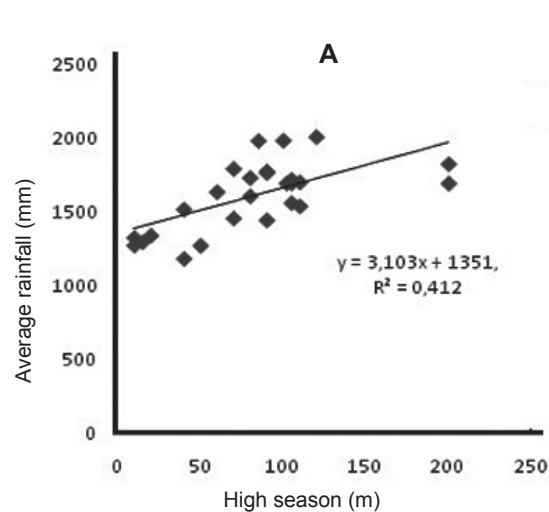
Per station, mean annual rainfall erosivity  $R$  values were calculated from monthly values  $R_m$ . Thus, Figure 9 shows the spatial distribution of mean annual  $R$  map (2) and b)  $R$  map (1), as well as mean annual rainfall and mean monthly  $R$  map (2) for the wet season (June-October) and the dry season (November-May)  $R$  (1); the spatial and temporal behavior was seemed in those months.

Table III shows mean annual  $P$  and mean annual  $R$  for the different rainfall stations in the watershed.

Within the basin, annual  $R$  ranges from a maximum of  $R$  (2) of 18,467  $MJ\cdot mm\cdot ha^{-1}\cdot h^{-1}$  at "San Laureano" station (number 145) to a minimum of 8,294  $MJ\cdot mm\cdot ha^{-1}\cdot h^{-1}$  in "Cuyaguaje" station (number 394) (Figure 10). For  $R$  (1), it has the same spatial behavior, the maximum value being at "San Laureano" with 22,044  $MJ\cdot mm\cdot ha^{-1}\cdot h^{-1}$  and the minimum value at "Cuyaguaje" with 9,673  $MJ\cdot mm\cdot ha^{-1}\cdot h^{-1}$ .



**Figure 6.  $R_m$  agreement between calculated and predicted values with the equations 10 and 12**



a) Height-Precipitation Relationship  
b) spatial distribution according to the north coordinate in the relationship Height-Precipitation

**Figure 7. Comparative diagrams between height and precipitation**

The authors (9) presented an overview of  $R$  value ranging from 10 studies at tropical sites around the world. Compared with those values, the lowest  $R$  value observed in our watershed of interest is among the largest of the minimum values observed in those studies.

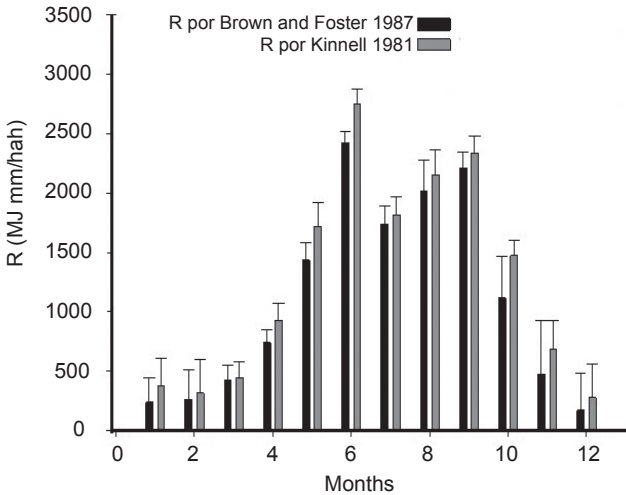
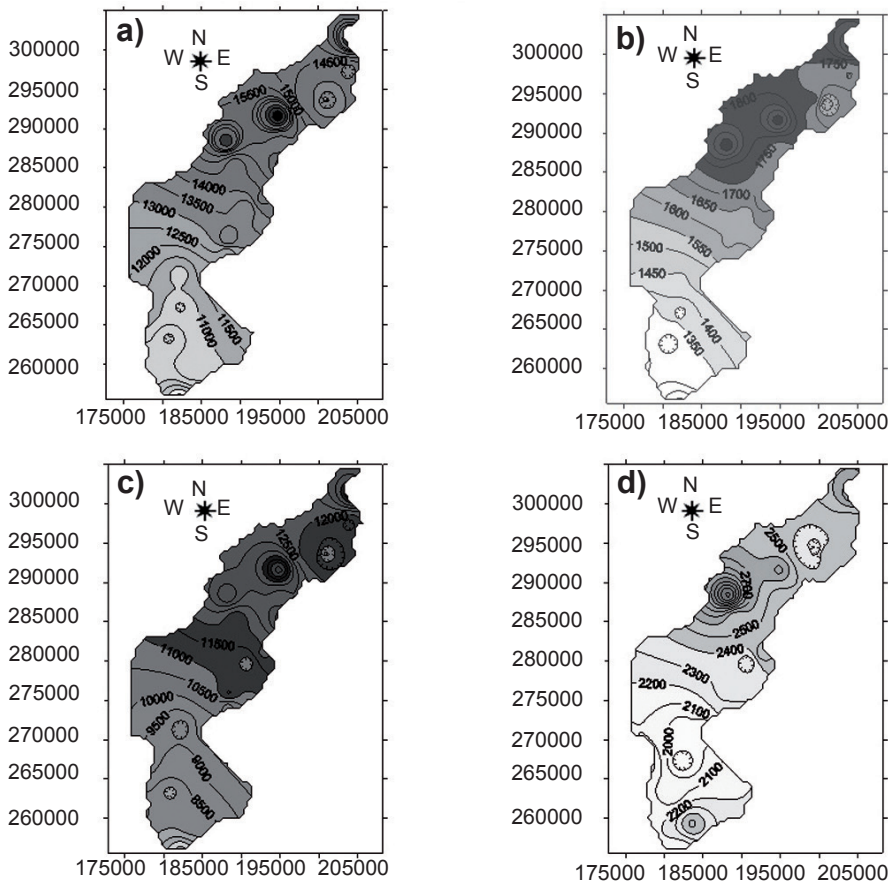


Figure 8. Monthly  $R$  by Kinnell and by Brown and Foster

Other large minimum  $R$  values were recorded in Columbian Andes (minimum  $R= 10,409 \text{ MJ mmha}^{-1} \text{ h}^{-1}$ ) and Malaysia (minimum  $R= 13,600 \text{ MJ mmha}^{-1} \text{ h}^{-1}$ ) (28). All other minimum values in that study did not exceed  $6345 \text{ MJ mmha}^{-1} \text{ h}^{-1}$ . Similarly, when considering our maximum  $R$  value, it belonged to the group with the largest values. In Malaysia, a value of  $21,600 \text{ MJ mmha}^{-1} \text{ h}^{-1}$  was recorded (28); in Hawaii, a value of  $23,828 \text{ MJ mmha}^{-1} \text{ h}^{-1}$  was presented (5) and in tropical Australia, a value of  $33,481 \text{ MJ mmha}^{-1} \text{ h}^{-1}$  was observed (29).

Other recent studies showed maximum  $R$  values of  $20,035 \text{ MJ mmha}^{-1} \text{ h}^{-1}$  in Brazil (30) and  $27,808 \text{ MJ mmha}^{-1} \text{ h}^{-1}$  in Nigeria (20).

Rainstorms with rainfall intensities below  $25 \text{ mm h}^{-1}$  are non-erosive (23). Such rain events of less than  $12,7 \text{ mm}$  should be omitted, unless at least  $6,35 \text{ mm}$  of rain falls in 15 minutes (7). Inspection of our records showed that only  $15,7 \%$  of events had an  $I_{30}$  of more than  $25 \text{ mm h}^{-1}$ , whereas  $26,3 \%$  of events showed rainfall amounts exceeding  $12,7 \text{ mm}$ .



a) Mean annual  $R$  by Brown and Foster values across the basin (2)  
 c) Mean monthly erosivity map in wet period by Brown and Foster (2)

b) Mean annual rainfalls  
 d) Mean monthly erosivity map in dry period by Brown and Foster (2)

Figure 9. Rainfall Erosivity Maps

**Table III. Mean Annual precipitation and R- RUSLE for each rainfall station**

Location	Station No.	Mean Annual Precipitation (mm)	Mean annual R (2) factor in MJ mm ha <sup>-1</sup>	Mean annual R (1) factor in MJ mm ha <sup>-1</sup>
La Catalina	3	1327,4	10817,9	12714,3
V Aniversario	122	1774,6	14003,9	15640,9
La Deseada	130	1518,6	13521,5	17609,5
Asiento Viejo	131	1298,5	11409,5	14504,2
Las Cañas	134	1458,3	11545,1	14197,1
Cayo Borrego	138	1561,4	12033,7	13384,1
Isabel Maria	140	1701,3	14096,7	16236,1
Quemado de Pineda	141	2006,6	18076,4	20761,3
Finca El Mulo	142	1694,4	14211,2	16626,4
Pica Pica	143	1764,2	14191,7	16210,3
José Martí	144	1693,5	16763,2	21865,3
San Laureano	145	1980,8	18467,0	22044,4
Santiago Puente	146	1982,8	17384,9	20579,7
Santa Lutgarda	148	1607,5	13959,2	16509,6
Correo San Carlos	246	1731,2	15154,1	19221,4
Correo Punta de la Sierra	247	1635,3	13034,3	15590,0
Isabel Rubio	248	1275,5	9877,0	11238,9
La Majagua	290	1718,8	14660,1	17127,7
Los Aguados	291	1694,4	13763,4	16380,6
E,A, Portales II	334	1445,8	10683,9	12270,0
Guane	342	1341,7	10410,2	11596,2
E,A, La Guira	354	1792,4	14116,0	15639,8
Sumidero	359	1540,4	12843,4	15362,2
Puesto de Mando D,A,P	368	1274,7	9978,5	11638,8
Granja Moncada	384	1824,3	14907,4	17067,5
Cuyaguaje E,C,	394	1185,6	8294,6	9673,7

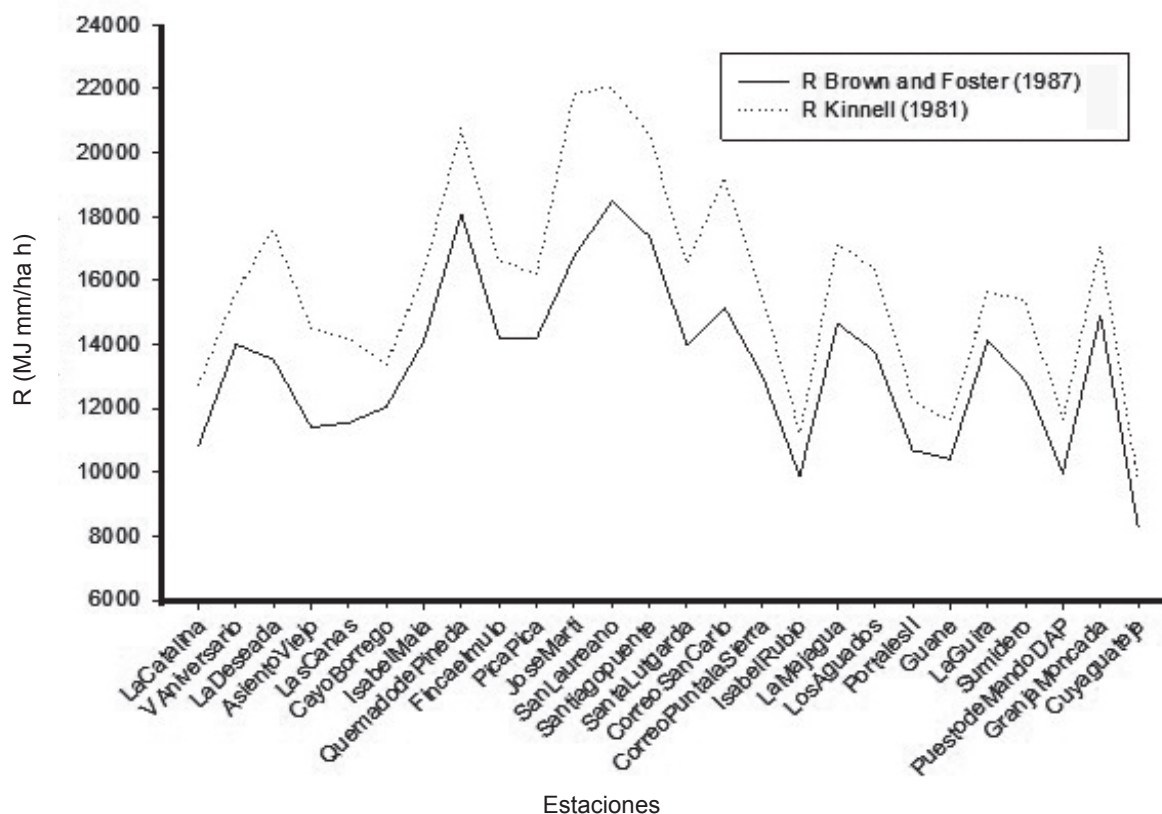


**Figure 10. Comparison between R yearly mean for de 26 stations by Kinnell and Brown and Foster**



This means that in our watershed of interest, most rains are non-erosive, but a minority of events is extremely erosive rendering those high annual erosivity values. In the previous section, we discussed that, for instance, rains (23) were less erosive than in our watershed.

Our highest  $R$  value of over  $22,000 \text{ MJ mm ha}^{-1} \text{ h}^{-1}$  (1) was observed at “San Laureano” (station 145), where annual precipitation was  $1980,8 \text{ mm}$ . In tropical Australia, for a similar amount of annual  $P$ ,  $R$  was much lower. On the contrary, in humid Nigeria, similar annual  $P$  values rendered similar erosivity values.

This shows that within tropical zones, large differences exist in the erosive power of rainstorms. Anyhow, annual  $R$  (2) was also well correlated with annual  $P$  ( $r= 0,94$ ).

Figure 9 a) shows that mean annual rainfall erosivity decreases with distance to the river mouth in the Caribbean Sea, that is, as we are moving away from the higher altitudes.

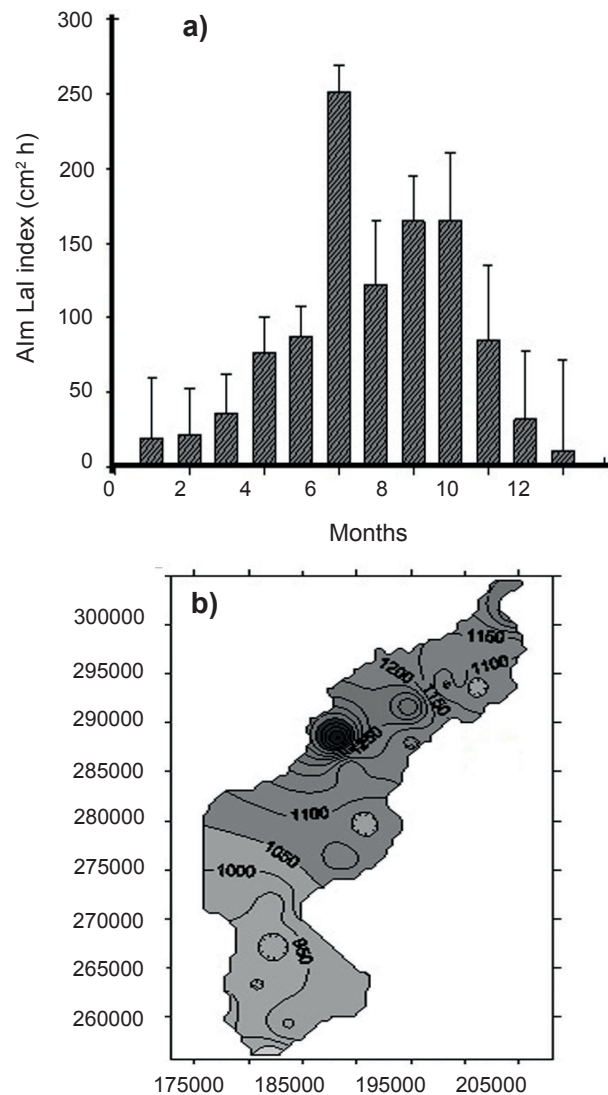
“San Laureano” station, where the highest  $R$  value was observed, is located in this higher part, but according to Table I, this station is not the highest, because it has  $85 \text{ m}$ . The behavior is not so uniform and evident between altitude and erosivity in this watershed.

On the other hand, “Cuyaguaje” station with the lowest  $R$  value is at the lower watershed part.  $R$  (2) values observed along the basin show an average value of  $12,895 \text{ MJ mm ha}^{-1} \text{ h}^{-1}$  with a 20 % of variation coefficient and  $R$  (1) has an average value of  $15,834 \text{ MJ mm ha}^{-1} \text{ h}^{-1}$  with a 23 % of variation coefficient. According to the classification of erosivity reported (31, 32) in Table IV, most of “Cuyaguaje” river basin has a very strong erosivity. Taking into account the distribution of  $R$  values within the basin, around 96 % of its area is affected by very strong rainfall erosivity.

**Table IV. Classification of rainfall erosivity R**

Range of $R$ values	Classification
$\leq 2452$	low erosivity
2452-4905	medium erosivity
4905-7357	medium-strong erosivity
7357-9810	strong erosivity
$> 9810$	very strong erosivity

Mean values of monthly Lal index  $AI_m$  changed approximately in the same way as mean monthly  $R$  index (Figure 11a). The correlation coefficient between monthly  $R$  (2) and monthly  $AI_m$  was  $0,96$  and with  $R$  (1) was  $0,97$  (Table V).



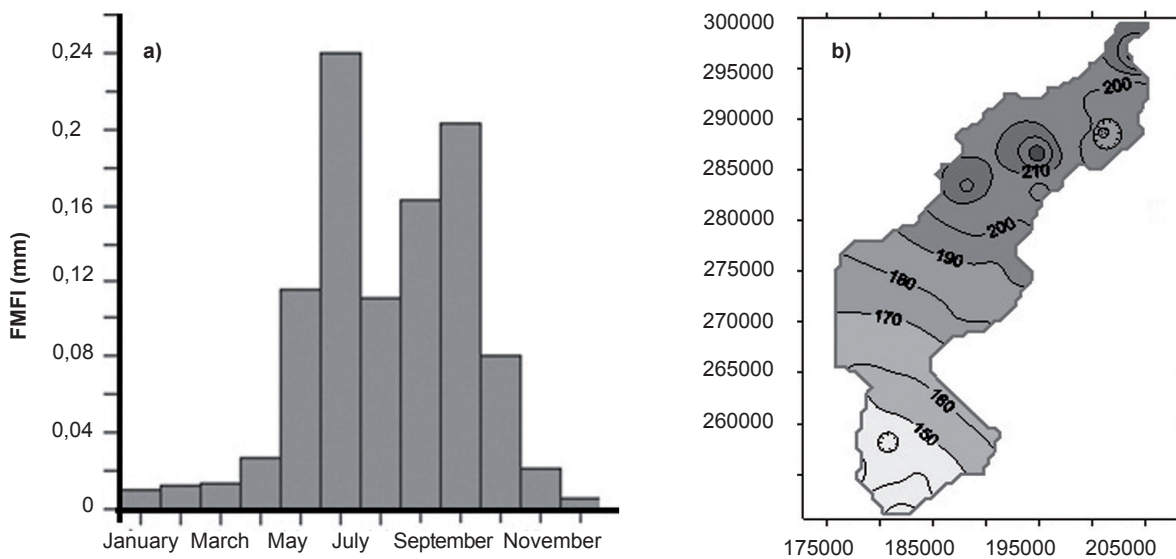
a) Mean monthly values of Lal index  
b) spatial distribution of mean annual values in  $\text{cm}^2 \text{ h}^{-1}$

**Figure 11. Lal index analysis**

The highest  $AI_m$  value in watershed was  $251,3 \text{ cm}^2 \text{ h}^{-1}$  for June, and the lowest value observed in December was  $11,6 \text{ cm}^2 \text{ h}^{-1}$ . Spatially, “Santiago Puente” (station 146) with the highest mean annual erosivity according to the maximum rainfall intensity at seven minutes was with  $1,659 \text{ cm}^2 \text{ h}^{-1}$  and located at the northern part of the basin. The lowest value was  $790 \text{ cm}^2 \text{ h}^{-1}$  at “Cuyaguaje” (station 394), located in the south of a flatter region (Figure 10). Spatial distribution of Lal index along the watershed is shown in Figure 11b). Regarding modified Fournier index (23), MFI, again the highest values were found in June ( $\text{MFI}= 0,240 \text{ mm}$ ) and the lowest ones in December ( $\text{MFI}= 0,005 \text{ mm}$ ) in the watershed (Figure 12 a). MFI correlated well with  $R$  (2)  $r= 0.97$  and with  $R$  (1)  $r= 0,98$ .

**Table V. Correlation coefficients obtained between temporal (monthly) indexes and spatial indexes considering mean annual values**

Correlation between	r value
Monthly R by Kinnell and monthly $AI_m$ values	0,97
Monthly R by Brown and Foster and monthly $AI_m$ values	0,96
Monthly R by Kinnell and monthly FMI values	0,98
Monthly R by Brown and Foster and monthly FMI values	0,97
Mean annual R by Brown and Foster and mean annual $AI_m$ values	0,87
Mean annual R by Kinnell and mean annual $AI_m$ values	0,90
Mean annual R by Brown and Foster and mean annual FMI values	0,95
Mean annual R by Kinnell and mean annual FMI values	



a) Mean monthly values of Modified Founier index (left)      b) spatial distribution of FMI (right)

**Figure 12. Modified Founier index analysis**

Spatially, mean annual MFI values showed its maximum value (230 mm) at “Quemado de Pineda” (station 141) and its minimum (99 mm) at “Cuyaguajeje” (station 394). This corresponds with the north and south of the basin respectively. The distribution of mean annual MFI within the watershed is shown in Figure 12b.

**CONCLUSIONS**

◆ It is first time in this basin and in the west part of Cuba that a deep study of rainfall erosivity is carried out, a very important step in any erosion research. This research work is necessary to successive erosion works in the area.

◆ It locates the most rainfall aggressiveness areas, to make further protection measures. Around 96 % of “Cuyaguajeje” watershed is affected by very strong erosivity related with the amount and intensities of rainfall in the basin. Mean annual R values obtained varies between 8200 and 18000 MJ mm ha<sup>-1</sup> h<sup>-1</sup> yr<sup>-1</sup> (2), kinetic energy equation and varies between 900 MJ mm ha<sup>-1</sup> h<sup>-1</sup> yr<sup>-1</sup> and 22000 MJ mm ha<sup>-1</sup> h<sup>-1</sup> yr<sup>-1</sup>. Values were very high in relation to other countries, whose climatic conditions are very different from Cuba, for instance, Belgium and Portugal with 860 MJ mm ha<sup>-1</sup> h<sup>-1</sup> yr<sup>-1</sup> and 3741.8 MJ mm ha<sup>-1</sup> h<sup>-1</sup> yr<sup>-1</sup> respectively.

◆ The regression equations obtained above for “V Aniversario” station were validated for “Portales II” (station localized in watershed south part), to calculate erosivity for 26 watershed stations, making use of daily amount of precipitations, demonstrating the truthfulness and applicability of the proposed methodology.

- ◆ In relation with distribution according to the year, mean monthly erosivity reaches the highest values in June with  $R(2) = 2423.1 \text{ MJ}\cdot\text{mm}\cdot\text{ha}^{-1}\cdot\text{h}^{-1}$  whereas December the lowest with  $R(2) = 171.1 \text{ MJ}\cdot\text{mm}\cdot\text{ha}^{-1}\cdot\text{h}^{-1}$ ,  $R(1) = 2748 \text{ MJ}\cdot\text{mm}\cdot\text{ha}^{-1}\cdot\text{h}^{-1}$  and  $R(1) = 279 \text{ MJ}\cdot\text{mm}\cdot\text{ha}^{-1}\cdot\text{h}^{-1}$  respectively. It was determined that there exists a high correspondence between mean monthly R factor and Alm and MFI indexes with higher correlation than 0,90.
- ◆ The spatial distribution of all the erosivity indexes studied varies from higher values at the northeast to lower values at the southwest of the basin, but the high (m) is not a determining factor in the rainfall behavior with correlation between both 0.41.

## ACKNOWLEDGEMENTS

The research work was conducted in the framework of the project UGENT-ZEIN 2005PR306 funded by Flemish Interuniversity Council-University Development Cooperation (VLIR), Belgium, to which we are greatly grateful.

## BIBLIOGRAPHY

1. Kinnell, P. I. A. "Rainfall Intensity-Kinetic Energy Relationships for Soil Loss Prediction". *Soil Science Society of America Journal*, vol. 45, no. 1, 2/01 de 1981, pp. 153-155, ISSN 0361-5995, DOI 10.2136/sssaj1981.03615995004500010033x.
2. Brown, L. C. y Foster, G. R. "Storm erosivity using idealized intensity distributions". *Transactions of the American Society of Agricultural Engineers*, vol. 30, no. 2, 1987, pp. 379-386, ISSN 0001-2351, 2151-0059.
3. Bandyopadhyay, S.; Ghosh, K. y Kumar, D. S. "A proposed method of bank erosion vulnerability zonation and its application on the River Haora, Tripura, India". *Geomorphology*, vol. 224, 1 de noviembre de 2014, pp. 111-121, ISSN 0169-555X, DOI 10.1016/j.geomorph.2014.07.018.
4. Schiettecatte, W.; D'hondt, L.; Cornelis, W. M.; Acosta, M. L.; Leal, Z.; Lauwers, N.; Almoza, Y.; Alonso, G. R.; Díaz, J.; Ruíz, M. y Gabriels, D. "Influence of landuse on soil erosion risk in the Cuyaguatete watershed (Cuba)". *CATENA*, vol. 74, no. 1, 15 de junio de 2008, pp. 1-12, ISSN 0341-8162, DOI 10.1016/j.catena.2007.12.003.
5. Renard, K. G. *Predicting Soil Erosion by Water: A Guide to Conservation Planning with the Revised Universal Soil Loss Equation (RUSLE)*. edit. U.S. Department of Agriculture, Agricultural Research Service, Washington, DC, 1997, 412 p., ISBN 978-0-16-048938-9.
6. Litschert, S. E.; Theobald, D. M. y Brown, T. C. "Effects of climate change and wildfire on soil loss in the Southern Rockies Ecoregion". *CATENA*, vol. 118, julio de 2014, pp. 206-219, ISSN 0341-8162, DOI 10.1016/j.catena.2014.01.007.
7. Wischmeier, W. H. y Smith, D. D. *Predicting rainfall erosion losses - a guide to conservation planning*. (ser. Agriculture Handbooks (USA), no. ser. 537), edit. USDA, Washington, DC, 1978, 62 p., CABDirect2, Record Number 19786726437.
8. Rivera, T. F.; Pérez, N. S.; Ibáñez, C. L. A. y Hernández, S. F. R. "Aplicabilidad del modelo SWAT para la estimación de la erosión hídrica en las cuencas de México". *Agrociencia*, vol. 46, no. 2, marzo de 2012, pp. 101-105, ISSN 1405-3195.
9. Stroosnijder, L. "Measurement of erosion: Is it possible?". *Catena*, vol. 64, 2005, pp. 162-173, ISSN 0341-8162.
10. Lal, R. *Soil Erosion Research Methods*. edit. CRC Press, 1 de mayo de 1994, 356 p., ISBN 978-1-884015-09-0.
11. Salles, C.; Poesen, J. y Sempere-Torres, D. "Kinetic energy of rain and its functional relationship with intensity". *Journal of Hydrology*, vol. 257, no. 1-4, 1 de febrero de 2002, pp. 256-270, ISSN 0022-1694, DOI 10.1016/S0022-1694(01)00555-8.
12. van Dijk, A. I. J. M.; Bruijnzeel, L. A. y Rosewell, C. J. "Rainfall intensity-kinetic energy relationships: a critical literature appraisal". *Journal of Hydrology*, vol. 261, no. 1-4, 15 de abril de 2002, pp. 1-23, ISSN 0022-1694, DOI 10.1016/S0022-1694(02)00020-3.
13. Rosewell, C. J. "Rainfall Kinetic Energy in Eastern Australia". *Journal of Climate and Applied Meteorology*, vol. 25, no. 11, 1 de noviembre de 1986, pp. 1695-1701, ISSN 0733-3021, DOI 10.1175/1520-0450(1986)025<1695:RKEIEA>2.0.CO;2.
14. Smith, J. A. y De Veaux, R. D. "The temporal and spatial variability of rainfall power". *Environmetrics*, vol. 3, no. 1, 1 de enero de 1992, pp. 29-53, ISSN 1099-095X, DOI 10.1002/env.3170030103.
15. Arnoldus, H. M. J. "Methodology used to determine the maximum potential average annual soil loss due to sheet and rill erosion in Morocco". *FAO Soils Bulletins (FAO)*, no. 34, 1977, pp. 39-51.
16. Lal, R. "Soil erosion on Alfisols in Western Nigeria: III. Effects of rainfall characteristics". *Geoderma*, vol. 16, no. 5, diciembre de 1976, pp. 389-401, ISSN 0016-7061, DOI 10.1016/0016-7061(76)90003-3.
17. Ramos, M. C. "Rainfall distribution patterns and their change over time in a Mediterranean area". *Theoretical and Applied Climatology*, vol. 69, no. 3-4, septiembre de 2001, pp. 163-170, ISSN 0177-798X, 1434-4483, DOI 10.1007/s007040170022.
18. Grauso, S.; Diodato, N. y Verrubbi, V. "Calibrating a rainfall erosivity assessment model at regional scale in Mediterranean area". *Environmental Earth Sciences*, vol. 60, no. 8, 22 de septiembre de 2009, pp. 1597-1606, ISSN 1866-6280, 1866-6299, DOI 10.1007/s12665-009-0294-z.
19. Diodato, N. y Bellocchi, G. "Environmental implications of erosive rainfall across Mediterranean". En: eds. Halley G. T. y Fridian Y. T., *Environmental impact assessments*, edit. NOVA Publishers, New York, USA, 2010, pp. 75-101, ISBN 0-08-02-215900.
20. Salako, F. K. "Development of isoerodent maps for Nigeria from daily rainfall amount". *Geoderma*, vol. 156, no. 3-4, 15 de mayo de 2010, pp. 372-378, ISSN 0016-7061, DOI 10.1016/j.geoderma.2010.03.006.

21. Abbaspour, K. C.; Faramarzi, M.; Ghasemi, S. S. y Yang, H. "Assessing the impact of climate change on water resources in Iran". *Water Resources Research*, vol. 45, no. 10, 1 de octubre de 2009, ISSN 1944-7973, DOI 10.1029/2008WR007615, [Consultado: 27 de enero de 2016], Disponible en: <<http://onlinelibrary.wiley.com/doi/10.1029/2008WR007615/abstract>>.
22. Asadi, H.; Rouhipour, H.; Rafahi, H. G. y Ghadiri, H. "Testing a Mechanistic Soil Erosion Model for Three Selected Soil Types from Iran". *Journal of Agricultural Science and Technology*, vol. 10, no. 0, 27 de enero de 2010, pp. 79-91, ISSN 1680-7073.
23. Mati, B. M.; Morgan, R. P.; Gichuki, F. N.; Quinton, J. N.; Brewer, T. R. y Liniger, H. P. "Assessment of erosion hazard with the USLE and GIS: A case study of the Upper Ewaso Ng'iro North basin of Kenya". *International Journal of Applied Earth Observation and Geoinformation*, vol. 2, no. 2, 2000, pp. 78-86, ISSN 0303-2434, DOI 10.1016/S0303-2434(00)85002-3.
24. Angima, S. D.; Stott, D. E.; O'Neill, M. K.; Ong, C. K. y Weesies, G. A. "Soil erosion prediction using RUSLE for central Kenyan highland conditions". *Agriculture, Ecosystems & Environment*, vol. 97, no. 1-3, julio de 2003, pp. 295-308, ISSN 0167-8809, DOI 10.1016/S0167-8809(03)00011-2.
25. Martinez, D. y Gori, E. G. "Raindrop size distributions in convective clouds over Cuba". *Atmospheric Research*, vol. 52, no. 3, septiembre de 1999, pp. 221-239, ISSN 0169-8095, DOI 10.1016/S0169-8095(99)00020-4.
26. FAOclim. *World-Wide Agroclimatic Data Base*. versión 2.02, [Windows 95/98/NT 4/2000/XP], 2003.
27. Mueller, E. A. *Raindrop distributions at Miami, Florida*. edit. Illinois State Water Survey, Meteorological Laboratory, University of Illinois, Urbana, 1962, 281 p.
28. Yu, B.; Hashim, G. M. y Eusof, Z. "Estimating the R-factor with limited rainfall data: A case study from Peninsular Malaysia". *Journal of Soil and Water Conservation*, vol. 56, no. 2, 4 de enero de 2001, pp. 101-105, ISSN 0022-4561, 1941-3300.
29. Yu, B. "Rainfall erosivity and its estimation for Australia's tropics". *Australian Journal of Soil Research*, vol. 36, no. 1, 1 de enero de 1998, pp. 143-166, ISSN 0004-9573.
30. da Silva, A. M. "Rainfall erosivity map for Brazil". *CATENA*, vol. 57, no. 3, 22 de agosto de 2004, pp. 251-259, ISSN 0341-8162, DOI 10.1016/j.catena.2003.11.006.
31. Carvalho, N. de O. *Hidrossedimentologia prática* [en línea]. 2.ª ed., edit. Interciencia, 1994, 372 p., [Consultado: 1 de febrero de 2016], Disponible en: <[https://books.google.com.br/books/about/Hidrossedimentologia\\_pr%C3%A1tica.html?hl=pt-BR&id=TP4cHQAACAAJ](https://books.google.com.br/books/about/Hidrossedimentologia_pr%C3%A1tica.html?hl=pt-BR&id=TP4cHQAACAAJ)>.
32. Winchell, M. F.; Jackson, S. H.; Wadley, A. M. y Srinivasan, R. "Extension and validation of a geographic information system-based method for calculating the Revised Universal Soil Loss Equation length-slope factor for erosion risk assessments in large watersheds". *Journal of Soil and Water Conservation*, vol. 63, no. 3, 5 de enero de 2008, pp. 105-111, ISSN 0022-4561, 1941-3300, DOI 10.2489/jswc.63.3.105.

Received: December 2<sup>nd</sup>, 2014

Accepted: October 29<sup>th</sup>, 2015